# Analysis of Peripapillary Geometric Characters in High Myopia Using Swept-Source Optical Coherence Tomography

Tomoko Asai,[1] Yasushi Ikuno,[1] Masahiro Akiba,[2] Tsutomu Kikawa,[2] Shinichi Usui,[1] and Kohji Nishida[1]

[1]Department of Ophthalmology, Osaka University Medical School, Osaka, Japan
[2]Topcon Corporation, Tokyo, Japan

Correspondence: Yasushi Ikuno, Department of Ophthalmology E7, Osaka University Medical School, 2-2 Yamadaoka, Suita, Osaka 565-0878, Japan;
yasushi.ikuno@gmail.com.

Submitted: June 17, 2015
Accepted: December 1, 2015

Citation: Asai T, Ikuno Y, Akiba M, Kikawa T, Usui S, Nishida K. Analysis of peripapillary geometric characters in high myopia using swept-source optical coherence tomography. *Invest Ophthalmol Vis Sci*. 2016;57:137–144. DOI:10.1167/iovs.15-17510

**Purpose.** We measured the three-dimensional geometric profile around the optic nerve head (ONH) using swept-source optical coherence tomography (SS-OCT) in highly myopic eyes.

**Methods.** We studied 114 highly myopic eyes (<−6.0 diopters [D]) of 114 patients without glaucoma. Eyes were examined using the prototype SS-OCT. The retinal pigment epithelium (RPE) and chorioscleral interface were traced, and the mean *y*-axis coordinates of 24 sectors were calculated in circular peripapillary (3.4-mm diameter) images. The peripapillary tilting index (PTI) was calculated by subtracting the mean *y*-axis coordinate of the RPE in a sector from the mean of all sectors. The main outcome measures were the PTI and its association with the staphyloma depth from the OCT images and the ovality index (OI) of the ONH and peripapillary atrophy (PPA) area from fundus photographs.

**Results.** The PTI differed significantly ($P < 0.0001$) among the 24 sectors and was lowest at the inferotemporal sector (−1930.76 μm). The minimal PTI value was in the temporal to inferotemporal sectors in 88 (77.2%) eyes and was correlated significantly with the OI ($P < 0.0001$) and age ($P < 0.001$) but not with the equivalent refractive error or axial length. The minimal PTI was correlated significantly with the PPA area ($P < 0.05$), minimal choroidal thickness ($P < 0.05$), macular choroidal thickness ($P < 0.0001$), and staphyloma depth ($P < 0.0001$).

**Conclusions.** The peripapillary area is tilted inferotemporally in 77.2% of myopic eyes. Peripapillary tilting was markedly greater in older patients. Greater tilt was associated with a thinner choroid, more extensive PPA, and deeper staphyloma.

Keywords: optical coherence tomography, myopia, optic nerve head, tilted disc

Based on epidemiologic studies, a higher prevalence of glaucoma is associated with the degree of myopia,[1,2] especially in Asian populations.[3,4] The higher susceptibility to glaucoma is hypothesized at a given IOP in myopic eyes from the conformational changes according to axial length (AL) elongation.[5] A variety of morphologic changes in highly myopic eyes have been documented using histology and optical coherence tomography (OCT), for example, flattening and enlargement of the optic disc,[6] lamina cribrosa or scleral thinning,[7] peripapillary atrophy (PPA) enlargement,[8] scleral deformation between the optic nerve head (ONH) and the macula,[9] and scleral pit formation inside the ONH or PPA,[10] some of which are believed to be partly responsible for increased susceptibility to glaucoma. However, the geometric analysis around the ONH in highly myopic eyes has not been well investigated.

Optic disc tilt and torsion are characteristic features of high myopia.[11] Tilted optic discs are characterized by two geometric variations: the apparent angle at which the optic nerve enters the eye, the so-called "oblique insertion" of the optic nerve, and rotation about the sagittal axis of the optic nerve. The prevalence of tilted discs has been associated with the degree of myopia.[12,13] Progressive tilting of the ONH with development of PPA in children according to myopic progression results from scleral stretching.[14] However, the correlation between optic tilt and glaucoma remains controversial.[13,15,16]

Recent advances in imaging technologies, such as swept-source OCT (SS-OCT), facilitate visualization of posterior deformities in highly myopic eyes.[17] Swept-source OCT has a longer wavelength light source and is as fast as 100,000 A-scans/second. These profiles enable longer and deeper scans compared to standard spectral-domain OCT and allow reconstruction of the posterior eye morphology in high myopia, which is highly curved and often has deep staphyloma. Several biometric parameters are being investigated to discern the specific ocular shape that will identify the underlying pathologies in myopia-related diseases.[9,18]

The aims of the current study were to analyze morphologically the peripapillary region in highly myopic eyes and quantify the slope of the eye wall 360° around the ONH using a new SS-OCT algorithm. We also compared our new parameter to conventional parameters of tilted discs, the ratio of the minimal to the maximal diameter of the optic nerve, and the torsion angle to understand how the peripapillary shape is associated with disc appearance.

## Subjects and Methods

### Subjects

A retrospective review of 114 eyes of 114 highly myopic patients (spherical equivalent refractive error [SERE] exceeding –6 diopters [D] or AL exceeding 26 mm) was done. Each subject underwent a complete ophthalmic examination and SS-OCT (Topcon, Tokyo, Japan) at Osaka University Hospital, Osaka, Japan, between December 2010 and April 2013. The subjects were consecutive patients who were referred to the Department of Ophthalmology, Osaka University Hospital, Osaka, Japan, and provided written informed consent to participate in this study. Inclusion criteria were the absence of ophthalmic or systemic symptoms, macular abnormalities causing visual impairment found on nonmydriatic fundus photographs and OCT images, fundus visualization obscured by cataract, history of intraocular surgery except for cataract surgery, glaucomatous disc cupping reviewed by a glaucoma specialist (SU), general good health, and availability of good-quality SS-OCT images. If both eyes met the study criteria, one eye was chosen randomly. Five eyes with extensive PPA in which the RPE line could not be traced on OCT images and four eyes with a glaucomatous optic appearance were excluded. Ultimately, 114 eyes of 114 subjects were included. The institutional review board/ethics committee of the Osaka University Hospital approved the study, which was conducted according to the tenets of the Declaration of Helsinki.

### SS-OCT and Peripapillary Circle Scan

The detailed specifications of the SS-OCT were described previously.[17] Briefly, this OCT is based on SS technology with a scan speed of 100,000 A-scans/sec. The center wavelength of the light beam is 1050 nm, and the effective axial resolution is 8 μm in tissue. A trained examiner performed the 3.4-mm peripapillary circle scan centered on the ONH. If the image was not centered exactly on the ONH, the scan was repeated until the desired scan was obtained. The scan always started horizontally temporally and always progressed superiorly, temporally, and inferiorly in a counterclockwise fashion in the left eye or clockwise in the right eye. All sectors were referred to alphabetically in the order of the scan, that is, the first sector was named A, with the first 12 sectors named A to L. The opposite sectors were named A‘ to L‘ (Fig. 1). The 32 single B-scan images were averaged for better choroidal and scleral visualization. A masked, experienced clinician (TA) measured the choroidal thicknesses using the caliper function in the OCT viewer software.

### Structural Biometry Analysis Using OCT

The peripapillary slope was quantitated using customized software provided by Topcon. Hyperscattering of the RPE line and choriosclera interface (CSI) was traced automatically on the OCT images, and analyses were performed after dividing the image into 24 sectors. We checked all the B-scans, and manual adjustments were made if necessary. The choroidal thickness, defined as the vertical distance between the RPE and CSI, was obtained as described previously.[19]

Each sector was equivalent to a 15° sectorial scan (Figs. 1, 2A). The mean vertical position of the RPE in each of the 24 sectors obtained from the *y*-axis coordinate of the OCT image also was calculated, and the following peripapillary tilting parameter was calculated. The vertical distance in micrometers between a given sector and the mean RPE position of the overall sectors was obtained (namely, the peripapillary tilting index [PTI]; Fig. 2A). The PTI always was calculated by automatically subtracting the mean RPE height of each sector from the mean RPE height of all sectors. The PTI was expressed as a plus or minus value to reflect the relative position in relation to the averaged RPE plane. If the RPE position of interest was posterior to the average line, it was expressed as a minus value and if anterior, it was expressed as a plus value (Fig. 2A). The mean choroidal thickness of each of the 24 sectors was calculated.

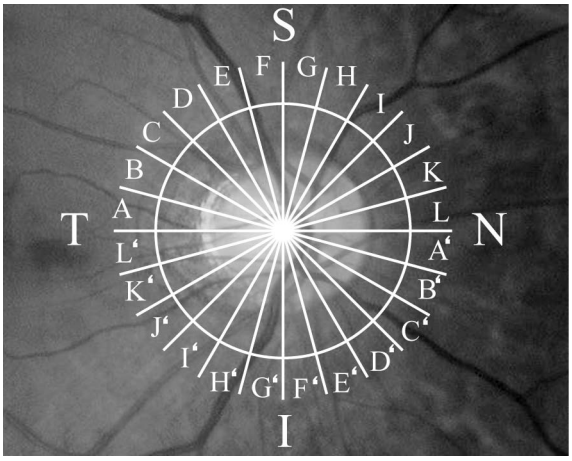


Figure 1. The sectors are named alphabetically in the first 12 sectors from A to L, as the OCT scan starts from temporally and proceeds nasally in a clockwise fashion in the right eyes and counterclockwise in the left eyes. The opposite sides of these 12 sectors are A‘ to L‘. S, superior; T, temporal; N, nasal; I, inferior.

The depth of the posterior staphyloma was determined according to the previously reported method.[20] The posterior staphyloma height was defined as the distance between the subfoveal RPE line and that between points 3 mm away from the fovea on both sides (nasal and temporal edge of the horizontal scan and superior and inferior vertical scan) including the fovea. The average of these four measurements was used as the height of the posterior staphyloma in this study (Fig. 2B).

### Other Examinations

An ophthalmic examination was performed simultaneously including measurement of the refractive error by automatic refractometry (Auto Ref/Keratometer ARK-530; Nidek Co., Ltd., Gamagori, Japan), IOP by noncontact tonometry (CT-90A, Topcon), AL by partial coherence interferometry (IOLMaster; Carl Zeiss Meditec, Dublin, CA), and color fundus photography through dilated pupils (TRC-50DX, Topcon). Color photographs of the optic disc were obtained and assessed morphometrically. The photographs were exported to ImageJ software (http://imagej.nih.gov/ij/; provided in the public domain by the National Institutes of Health, Bethesda, MD, USA), and the ratio of the maximal to minimal diameter (ovlity index [OI]), which was defined as tilted when less than 0.75,[13] and the degree of the maximal diameter to the vertical line (disc torsion) were measured (Fig. 3). Peripapillary atrophy was differentiated in a peripheral α zone characterized by irregular pigmentation and a β zone at the optic disc border, characterized by visible sclera and visible large choroidal vessels.[21] The magnification by the optical media was corrected according to Littmann's method,[22] which was calculated from fundus photographs by the refractive error and AL using image filing software (ImageNet; Topcon).

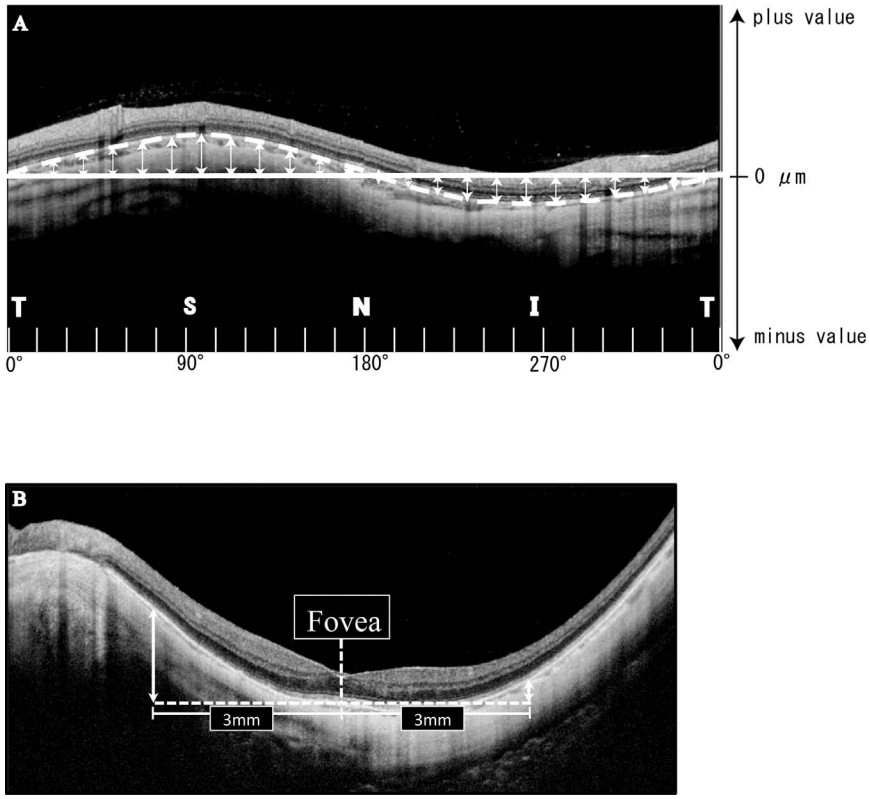


FIGURE 2. (**A**) Quantification of the peripapillary slope using SS-OCT with customized software. A circular peripapillary scan of 3.4 mm was obtained, and the RPE line is drawn automatically and sectored every 15°. The mean vertical position of the RPE in each sector is obtained (*dashed line*) and the vertical distance from the mean position (*solid line*) is calculated (*arrowheads*). The position is represented as a minus or plus value in relation to the mean RPE reference position. (**B**) The posterior staphyloma height was defined as the vertical distance from the RPE line beneath the fovea to 3 mm nasal, temporal, superior, and inferior from the horizontal and vertical B-scan including the fovea.

### Reproducibility Test

The intervisit reproducibility of the PTI was validated based on the OCT images from 10 normal healthy eyes (SERE, −2.10 ± 1.86 D; mean AL, 24.70 ± 0.95 mm; and mean age, 28.8 ± 2.8 years) twice on different days at 3 PM, and the intraclass correlation coefficients (ICCs) determined.

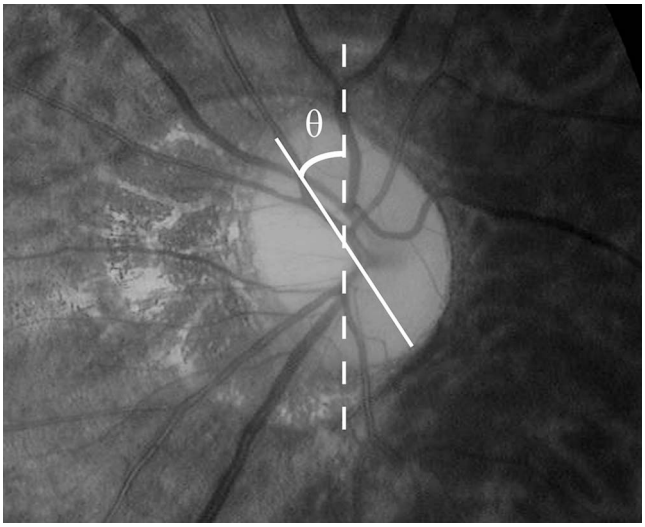


FIGURE 3. The degree of torsion is defined as the angle between the longest axis and the *vertical line*.

### Statistical Analysis

The obtained data were analyzed using the paired or unpaired *t*-test, univariate or multivariate regression analysis, and multiple variable analysis (JMP statistical software package, version 9.0; SAS Institute, Inc., Cary, NC, USA), with statistical significance defined as $P < 0.05$. The ICCs[23] were calculated using MedCalc (MedCalc Software, Ostend, Belgium). Eyes with an intraocular lens were excluded when analyzing correlations with refractive errors.

## RESULTS

A total of 114 eyes of 114 subjects with myopia (82 women, 32 men) met the inclusion criteria. The mean patient age was 54.7 ± 16.7 years (SD) years; range, 14–86 years). Of the eyes, 92 (81%) were phakic and 22 (19%) were pseudophakic. The mean SERE of the phakic eyes was −11.9 ± 0.43 D (range, −25 to −3.38); the mean AL of all eyes was 28.72 ± 1.68 mm (range, 25.09–33.51).

### PTI of Each Sector and Reproducibility

The mean PTI values of each sector (Fig. 4A) differed significantly ($P < 0.0001$, by 1-way ANOVA) among the 24 sectors. The mean PTI was the highest in sector K (1930.76 μm) and the lowest in sector K‘ (−1930.76 μm). The minimal PTI was located inferotemporally (G‘ to L‘ sectors) in 88 (77.2%) eyes (Fig. 4B). The reproducibility of the PTI was good (ICC, 0.8–0.9) in sectors A to G, I to L, A‘ to G‘, and I‘ to L‘. The ICCs of the other sectors were fair (ICC, 0.7–0.8).

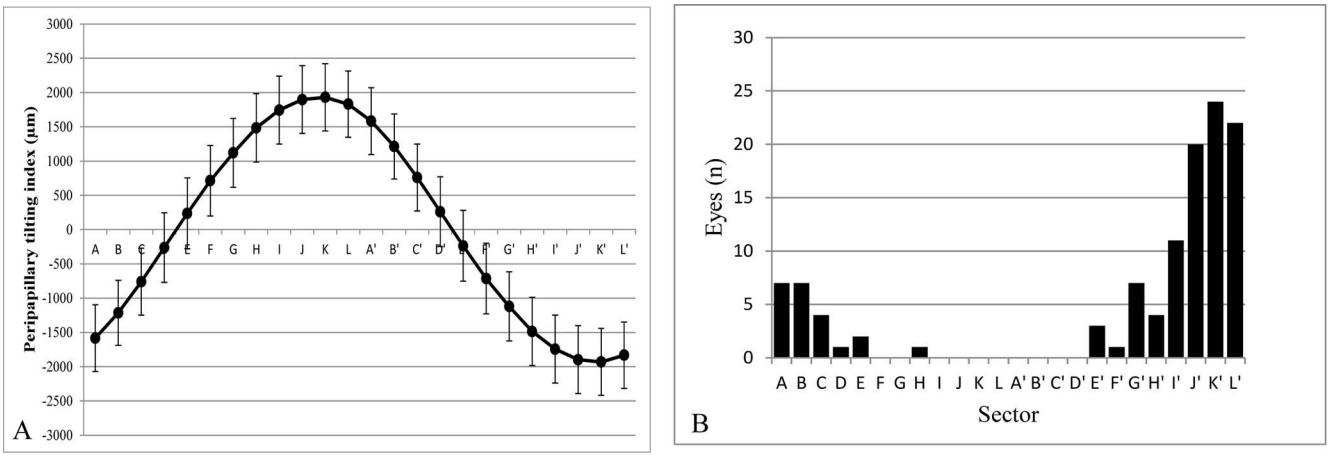


**Figure 4.** (**A**) The mean PTI values in all eyes. The PTI is highest in sector K and lowest in K', which differs significantly ($P < 0.0001$ by 1-way ANOVA). (**B**) The distribution of the sectors with the minimal PTI. The largest number of eyes with a minimal PTI value is in K'.

## Comparison Between PTI and Conventional Tilting Indices

The minimal PTI value was correlated significantly with the OI ($P < 0.0001$, $R^2 = 0.28$) but not with the degree of torsion ($P = 0.74$, $R^2 = 0.00$). The OI and degree of torsion also were not correlated ($P = 0.93$, $R^2 = 0.00$) with each other. The correlations among these factors and others are shown in Table 1. The minimal PTI value was associated significantly with age ($P < 0.001$), sex ($P < 0.01$), minimal choroidal thickness around the ONH ($P < 0.05$), PPA area ($P < 0.05$), macular choroidal thickness ($P < 0.0001$), and staphyloma depth ($P < 0.0001$). The OI showed a similar trend with significant associations with age ($P < 0.01$), minimal choroidal thickness around the ONH ($P < 0.05$), macular choroidal thickness ($P < 0.0001$), and staphyloma depth ($P < 0.0001$). However, none of the factors was associated significantly with the degree of torsion.

The correlations between the average PTI value of each sector and conventional tilting indices are shown in Table 2. The PTI was correlated significantly with the OI in all sectors except for the superotemporal sectors of D ($P = 0.78$) and E ($P = 0.18$). In contrast, torsion was correlated significantly with the PTI temporally to superotemporally (from A–G, and from A'–G') but not in the other sectors. The radar chart of the $R^2$ value of each sectors had a unique shape. The OI showed a relatively high $R^2$ value in the inferotemporal–superonasal direction (Fig. 5A); in contrast, the torsion had a high $R^2$ value in the superotemporal–inferonasal direction (Fig. 5B).

## Subgroup Analysis of Sectors Most Frequently Showing a Minimal PTI

Minimal PTI values were seen between the temporal and inferotemporal sectors (sectors B, A, L', K', J', and I', from superior to inferior; Fig. 4B) in 91 (79.8%) eyes. We reanalyzed the characteristics of these eyes to profile the location of sectors with a minimal PTI and other ophthalmologic factors (Fig. 6). The mean minimal PTI value ($P = 0.05$), OI ($P < 0.01$), and staphyloma depth ($P = 0.01$) differed significantly between sectors with a minimal PTI value. Interestingly, sector K' always had the smallest minimal PTI value, smallest OI, and highest posterior staphyloma.

# Discussion

## Rationale of Disc Tilting and Conventional Parameters

Oblique insertion of the optic nerve occurs typically and may indicate underlying mechanical stress on the ONH.[24] The OI, defined as the shortest/longest axis of the ONH on fundus photographs, is the gold standard to identify this "obliqueness" in myopic eyes. However, it was difficult to quantitate the level

**Table 1.** Correlation Between Three Tilting Indices and Various Factors in 114 Eyes with High Myopia

| | Minimum Peripapillary Tilting Index Value | | | Ovality Index | | | Torsion Degree | | |
|---|---|---|---|---|---|---|---|---|---|
| | *P* Value | Coefficient | $R^2$ | *P* Value | Coefficient | $R^2$ | *P* Value | Coefficient | $R^2$ |
| Age, y | <0.001* | −6.94 | 0.11 | <0.01* | −0.0028 | 0.07 | 0.25 | 0.19 | 0.01 |
| Men/women | <0.01† | – | – | 0.08 | – | – | 0.90 | – | – |
| Axial length, mm | 0.10 | 31.8 | 0.02 | 0.88 | 0.00 | 0.00 | 0.58 | −0.94 | 0.00 |
| SERE, phakic only, diopters | 0.61 | 3.99 | 0.00 | 0.44 | 0.01 | 0.00 | 0.51 | 0.48 | 0.00 |
| Minimal cpChT, μm | 0.04* | 1.6 | 0.04 | 0.02* | 0.00088 | 0.05 | 0.61 | 0.034 | 0.00 |
| PPA area, $mm^2$ | 0.02* | −13.0 | 0.05 | 0.63 | −0.0013 | 0.00 | 0.19 | −0.61 | 0.02 |
| Macular ChT, μm | <0.0001* | 1.72 | 0.14 | <0.0001* | 0.00086 | 0.14 | 0.26 | 0.05 | 0.01 |
| Depth of staphyloma, μm | <0.0001* | −0.65 | 0.20 | <0.0001* | −0.00041 | 0.32 | 0.93 | 0..001 | <0.01 |

cpChT, circumpapillary choroidal thickness; ChT, choroidal thickness.
* Significant by regression analysis.
† Significant by ANOVA.

**Table 2.** Correlation Between Peripapillary Tilting Index Value of Each Sector and Ovality Index or Torsion Degree of 114 Highly Myopic Eyes

| | Ovality Index | | | Degree of Torsion | | |
|---|---|---|---|---|---|---|
| Sector | Coefficient | *P* Value | $R^2$ | Coefficient | *P* Value | $R^2$ |
| A | 2908.6 | <0.0001* | 0.26 | 2.48 | 0.04* | 0.04 |
| B | 2069.9 | <0.0001* | 0.14 | 3.18 | <0.01* | 0.07 |
| C | 1141.1 | 0.04* | 0.04 | 3.67 | <0.01* | 0.08 |
| D | 156.5 | 0.78 | 0.00 | 3.85 | <0.01* | 0.08 |
| E | −773.5 | 0.18 | 0.02 | 3.80 | <0.01* | 0.08 |
| F | −1577.7 | <0.01* | 0.07 | 3.49 | <0.01* | 0.07 |
| G | −2166.6 | <0.0001* | 0.13 | 3.02 | 0.01* | 0.05 |
| H | −2636.9 | <0.0001* | 0.20 | 2.33 | 0.06 | 0.03 |
| I | −3144.2 | <0.0001* | 0.29 | 1.46 | 0.23 | 0.01 |
| J | −3526.4 | <0.0001* | 0.36 | 0.49 | 0.69 | 0.00 |
| K | −3646.5 | <0.0001* | 0.40 | −0.66 | 0.59 | 0.00 |
| L | −3425.2 | <0.0001* | 0.35 | −1.64 | 0.17 | 0.02 |

* Significant by regression analysis.

and direction of the maximal slope in a three-dimensional structure even with modern imaging modalities. The nasal elevation in comparison with the temporal counterpart can be an indirect measurement of this, and Heidelberg Retina Tomograph II ([HRT] Heidelberg Engineering, Heidelberg, Germany) studies have shown a significantly greater height variation in myopic eyes.[25,26]

However, issues remain. One is the wide variation in disc sizes in myopic eyes, which must introduce bias into the measurements of the top of the rims and the comparisons of the contour. Wang et al.[27] reported that the disc areas varied 1 to 7.6 times in a large Chinese cohort. The disc area increases with the degree of myopia; however, the curve is steep beyond −7 or −8 D of SERE. This indicates that the disc is markedly stretched in high myopia, and the morphologic parameters of the disc may be difficult to standardize. Another issue is that the direction with the steepest tilt cannot be represented by the OI, because this is a two-dimensional parameter. The papillomacular nerve fiber bundle often is damaged selectively in myopic eyes,[28] and knowing the steepest direction of the disc may be worthwhile to search for high risk groups.

## Reproducibility of the PTI

The reproducibility was excellent between the different days in most sectors, indicating that the PTI can be used as a parameter of the tilting of the ONH. Regarding the other glaucoma parameters used in daily glaucoma practice, the retinal nerve fiber thickness has been typically reported to have an excellent ICC of greater than 90%.[29,30] Tan et al.[31] reported the average retinal nerve fiber layer (RNFL) and the RNFL in the superior, inferior, and temporal quadrants, with ICCs ranging from 0.859 to 0.908. The nasal quadrant had a lower ICC of 0.663. Those investigators mentioned that Blumenthal et al.[32] and Jones et al.[33] previously had reported poorer repeatability in the nasal quadrants using the OCT2 and concluded that the poorer ICC in the nasal quadrant may be unique to the equipment manufacturer. We believe this ICC of the PTI is acceptable for use in a clinical setting. However, the reproducibility was very poor between the lower nasal and upper temporal sectors, for which the reason was unclear. If the reproducibility is not good in these locations, the PTI must be interpreted carefully. The effects of head tilting and fixation also must be considered.

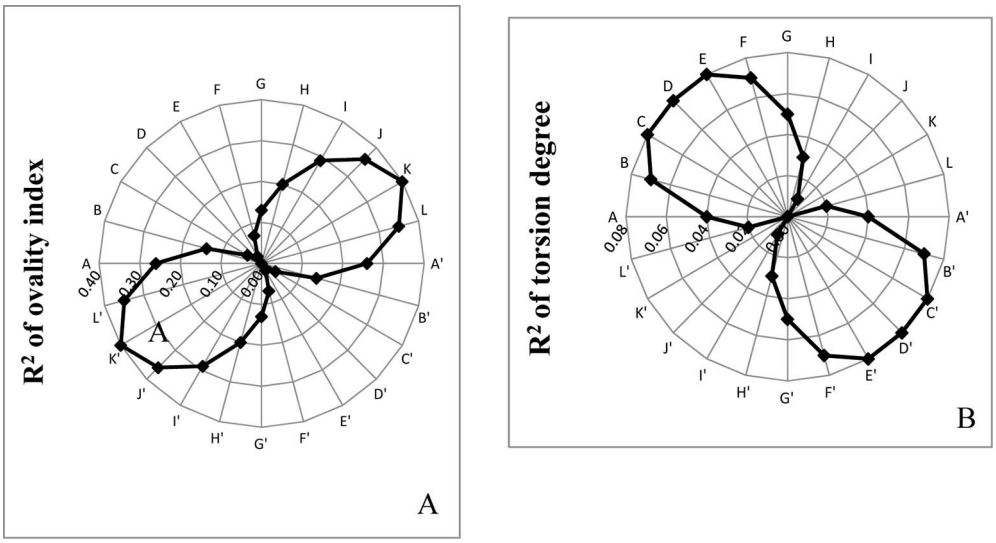


**Figure 5.** The $R^2$ values between (**A**) the OI and (**B**) the degree of torsion and the PTI values in each sector. The OI has a relatively high $R^2$ value in the inferotemporal–superonasal direction; in contrast, torsion does not have a high $R^2$ value in the superotemporal–inferonasal direction, which is perpendicular to the OI.

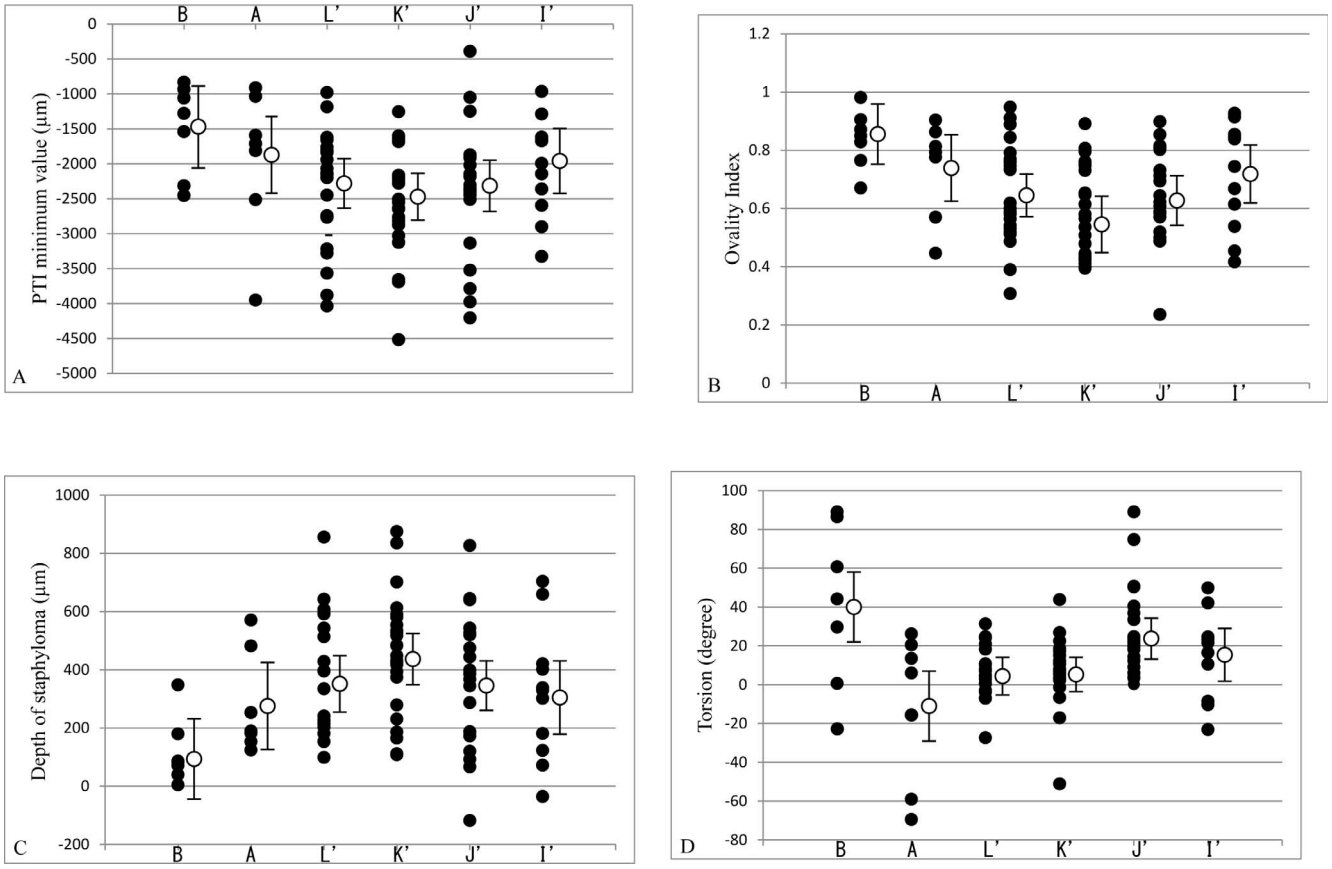


**Figure 6.** The subgroup analysis of sectors shows a minimal PTI value most frequently. (**A**) The minimal PTI value, (**B**) OI, (**C**) staphyloma depth, (**D**) angle of torsion, and the sectors with the minimal PTI values. The *open circles* indicate the mean number. *Error bars*: standard deviation.

## Agreement of PTI With OI and Degree of Torsion

The association between the PTI value in each sectors and OI differed among the sectors. The current results showed that the inferotemporal sectors generally were more highly associated with the OI. This finding suggested that the OI, the conventional tilting parameter, mostly represented the slope from superonasally to inferotemporally; however, the OI did not reflect tilting toward other directions, for example, inferonasally to superotemporally. Similar findings have been reported using the HRT3, and one study reported that the OI was correlated significantly with horizontal tilt measured by three-dimensional HRT imaging but not with vertical tilt,[26] which agreed with the current data.

The current study also showed that the PTI had the highest correlation with torsion in the superotemporal–inferonasal sectors and superior–interior sectors. Interestingly, these directions are on the perpendicular axis against the sectors with a high correlation with the OI. The OI mainly represents the tilting degree in the superonasal to inferotemporal direction, while the degree of torsion represents the tilting degree in the inferonasal to superotemporal direction. However, the $R^2$ values were normally smaller in the degree of torsion than the OI. Therefore, the degree of torsion is not as closely related to the PTI as is the OI.

## Relationship of PTI to Staphyloma and PPA Area

We found a close correlation between the staphyloma depth and the minimal PTI value, indicating that peripapillary tilting is associated closely with staphyloma formation. In other words, peripapillary deformity mainly results from posterior protrusion. A strong correlation also was found between the minimal PTI value and the PPA area. The myopic disc deviates from temporally to nasally with myopia progression.[11] Age was associated with the minimal PTI value. Interestingly, older patients tended to have a minimal PTI value in the inferior sector. Peripapillary atrophy enlargement based on myopic progression also was observed in children.[14] Taken together, the peripapillary area tilts according to the posterior staphyloma protrusion at the macula and the PPA consequently enlarges.

## Peripapillary Choroidal Thickness and Minimal PTI Sector

The current results showed that the mean peripapillary choroidal thickness in myopic eyes ranged from 56.1 μm (J', inferotemporal sector) to 104.5 μm (L, nasal sector). We found that the inferotemporal sectors of the peripapillary choroid were thinner than the other sectors, which agreed with previous studies that reported that the inferior (or inferotemporal) sector had a thinner choroid.[34] This area corresponded to the area in which the PTI value was lowest. In other words, the choroid became thinner at the point at which the disc tilt deviated. The choroidal thickness also coincided with the PPA area and staphyloma depth. These results all agreed with the conventional hypothesis that AL elongation in myopic eyes stretches the posterior eye wall, causing choroidal thinning around the ONH.

## Minimal PTI Value and Myopic Parameters

It is noteworthy that the PTI and OI were not correlated with the SERE or AL, which agreed in part with previous reports. One

study of 137 eyes with a mean SERE of −6.30 ± 3.70 D reported a significant ($P < 0.01$) correlation with the AL (Pearson's correlation coefficient, −0.22).[12] However, there were differences in the patient demographic data between their study and the current study. The current study included subjects with a mean SERE of −10.0 D and the mean ages were, respectively, 21.1 and 54.1 years. The agreement with these studies likely indicates that disc tilting is affected by local protrusion of the eye ball rather than general global enlargement.

## Direction of Tilting and Other Factors in Subgroup Analysis

The PTI was significantly higher in the lower temporal sectors, which indicated that the ONH in myopic eyes tends to tilt in that direction. Subgroup analysis of a group with temporal to inferotemporal tilting showed that the minimal PTI value was lowest when the minimal sector was K' (Fig. 6). The value increased gradually in the subsequent sectors, suggesting that a high degree of tilting occurs in the inferotemporal direction. Interestingly, the tilting in the lower sectors was associated with an older mean age, which may suggest that the greatest tilting may shift inferiorly according to age. However, since the current study was not longitudinal, further study is needed.

## Study Limitations

The current study had a small number of subjects. In addition, we excluded some subjects with marked PPA because we could not trace the RPE line. Therefore, there is a possibility of age-related bias. Another investigation with more subjects is needed. As our subjects did not have glaucoma, no conclusion concerning the association between myopic optic tilt and glaucoma can be made. Examination artifacts, such as head tilting, cannot be ruled out. Finally, PTI is a parameter of the peripapillary structure and does not represent disc tilting.

## *Acknowledgments*

Disclosure: **T. Asai**, None; **Y. Ikuno**, None; **M. Akiba**, Topcon Corporation (E); **T. Kikawa**, Topcon Corporation (E); **S. Usui**, None; **K. Nishida**, None

## *References*

1. Podos S, Becker B, Mortion W. High myopia and primary open-angle glaucoma. *Am J Ophthalmol*. 1966;62:1039–1043.
2. Mitchell P, Hourihan F, Sandbach J, et al. The relationship between glaucoma and myopia: the Blue Mountains Eye Study. *Ophthalmology*. 1999;106:2010–2015.
3. Xu L, Wang Y, Wang Y, et al. High myopia and glaucoma susceptibility. The Beijing Eye Study. *Ophthalmology*. 2007; 114:216–220.
4. Wong TY, Foster PJ, Hee J, et al. The prevalence and risk factors for refractive errors in adult Chinese residents in Singapore. *Invest Ophthalmol Vis Sci*. 2000;41:2486–2494.
5. Jonas JB, Budde WM. Optic nerve damage in highly myopic eyes with chronic open-angle glaucoma. *Eur J Ophthalmol*. 2005;15:41–47.
6. Jonas JB, Gusek GC, Naumann GO. Optic disk morphometry in high myopia. *Graefes Arch Clin Exp Ophthalmol*. 1988;226: 587–590.
7. Jonas JB, Berenshtein E, Holbach L. Lamina cribrosa thickness and spatial relationships between intraocular space and cerebrospinal fluid space in highly myopic eyes. *Invest Ophthalmol Vis Sci*. 2004;45:2660–2665.
8. Hayashi K, Tomidokoro A, Lee KY, et al. Spectral-domain optical coherence tomography of β-zone peripapillary atrophy: influence of myopia and glaucoma. *Invest Ophthalmol Vis Sci*. 2012;53:1499–1505.
9. Akagi T, Hangai M, Kimura Y, et al. Peripapillary scleral deformation and retinal nerve fiber damage in high myopia assessed with swept-source optical coherence tomography. *Am J Ophthalmol*. 2013;155:927–936.
10. Ohno-Matsui K, Akiba M, Moriyama M, et al. Acquired optic nerve and peripapillary pits in pathologic myopia. *Ophthalmology*. 2012;119:1685–1692.
11. Apple DJ, Rabb MF, Walsh PM. Congenital anomalies of the optic disc. *Surv Ophthalmol*. 1982;27:3–41.
12. Tay E, Seah SK, Chan SP, et al. Optic disc ovality as an index of tilt and its relationship to myopia and perimetry. *Am J Ophthalmol*. 2005;139:247–252.
13. How AC, Tan GS, Chan YH, et al. Population prevalence of tilted and torted optic discs among an adult Chinese population in Singapore: the Tanjong Pagar Study. *Arch Ophthalmol*. 2009;127:894–899.
14. Kim W, Kim M, Weinreb RN, et al. Optic disc change with incipient myopia of childhood. *Ophthalmology*. 2012;119:21–26.
15. Park HY, Lee K, Park CK. Optic disc torsion direction predicts the location of glaucomatous damage in normal-tension glaucoma patients with myopia. *Ophthalmology*. 2012;119: 1844–1851.
16. You QS, Xu L, Jonas JB. Tilted optic discs: the Beijing Eye Study. *Eye*. 2008;22:728–729.
17. Yasuno Y, Hong Y, Makita S, et al. In vivo high-contrast imaging of deep posterior eye by 1-μm swept source optical coherence tomography and scattering optical coherence angiography. *Opt Express*. 2007;15:6121–6139.
18. Ohno-Matsui K, Akiba M, Modegi T, et al. Association between shape of sclera and myopic retinochoroidal lesions in patients with pathologic myopia. *Invest Ophthalmol Vis Sci*. 2012;53: 6046–6061.
19. Ikuno Y, Kawaguchi K, Nouchi T, et al. Choroidal thickness in healthy Japanese subjects. *Invest Ophthalmol Vis Sci*. 2010; 51:2173–2176.
20. Ikuno Y, Tano Y. Retinal and choroidal biometry in highly myopic eyes with spectral-domain optical coherence tomography. *Invest Ophthalmol Vis Sci*. 2009;50:3876–3880.
21. Jonas JB, Nhung XN, Gusek GC, et al. The parapapillary chorio-retinal atrophy in normal and glaucoma eyes. I: morphometric data. *Invest Ophthalmol Vis Sci*. 1989;30: 908–918.
22. Littmann H. Determination of the real size of an object on the fundus of the living eye [in German]. *Klin Monbl Augenheilkd*. 1982;180:286–289.
23. Shrout PE, Fleiss JL. Intraclass correlations: uses in assessing rater reliability. *Psychol Bull*. 1979;86:420–48.
24. Chihara E, Sawada A. Atypical nerve fiber layer defects in high myopes with high-tension glaucoma. *Arch Ophthalmol*. 1990; 108:228–232.
25. Tsutsumi T, Tomidokoro A, Saito H, et al. Confocal scanning laser ophthalmoscopy in high myopic eyes in a population-based setting. *Invest Ophthalmol Vis Sci*. 2009;50:5281–5287.
26. Takasaki H, Higashide T, Takeda H, et al. Relationship between optic disc ovality and horizontal disc tilt in normal young subjects. *Jpn J Ophthalmol*. 2013;57:34–40.
27. Wang Y, Xu L, Zhang L, et al. Optic disc size in a population based study in northern China: the Beijing Eye Study. *Br J Ophthalmol*. 2006;90:353–356.
28. Kimura Y, Hangai M, Morooka S, et al. Retinal nerve fiber layer defects in highly myopic eyes with early glaucoma. *Invest Ophthalmol Vis Sci*. 2012;53:6472–6478.

29. González-García AO, Vizzeri G, Bowd C, et al. Reproducibility of RTVue retinal nerve fiber layer thickness and optic disc measurements and agreement with Stratus optical coherence tomography measurements. *Am J Ophthalmol*. 2009;147: 1067–1074.
30. Budenz DL, Fredette MJ, Feuer WJ, et al. Reproducibility of peripapillary retinal nerve fiber thickness measurements with stratus OCT in glaucomatous eyes. *Ophthalmology*. 2008;115: 661–666.
31. Tan BB, Natividad M, Chua KC, et al. Comparison of retinal nerve fiber layer measurement between 2 spectral domain OCT instruments. *J Glaucoma*. 2012;21:266–273.
32. Blumenthal EZ1, Williams JM, Weinreb RN, et al. Reproducibility of nerve fiber layer thickness measurements by use of optical coherence tomography. *Ophthalmology*. 2000;107: 2278–2282.
33. Jones AL, Sheen NJ, North RV, et al. The Humphrey optical coherence tomography scanner: quantitative analysis and reproducibility study of the normal human retinal nerve fibre layer. *Br J Ophthalmol*. 2001;85:673–677.
34. Ho J, Branchini L, Regatieri C, et al. Analysis of normal peripapillary choroidal thickness via spectral domain optical coherence tomography. *Ophthalmology*. 2011;118:2001–2007.

Investigative Ophthalmology & Visual Science